

# Dielectric, ac conductivity and electric modulus studies at MPS structure with (Cu<sub>2</sub>O-CuO)-doped PVA interfacial layer

A. BÜYÜKBAŞ-ULUŞAN<sup>a,\*</sup>, S. ALTINDAL YERİŞKİN<sup>b</sup>, A. TATAROĞLU<sup>a</sup>, M. BALBASI<sup>c</sup>,  
Y. AZIZIAN-KALANDARAGH<sup>d,e</sup>

<sup>a</sup>Department of Physics, Faculty of Sciences, Gazi University, Ankara, Turkey

<sup>b</sup>Department of Chemical Engineering, Faculty of Engineering, Gazi University, Ankara, Turkey

<sup>c</sup>Department of Chemical Engineering, Faculty of Engineering, Gazi University, Ankara, Turkey

<sup>d</sup>Department of Physics, Faculty of Sciences, University of Mohaghegh Ardabili, Ardabil, Iran

<sup>e</sup>Department of Engineering Sciences, Sabalan University of Advanced Technologies, Namin, Iran

We have investigated the ac conductivity, complex dielectric and modulus properties of Au/(Cu<sub>2</sub>O-CuO) doped-PVA/n-Si (MPS) structure. The parameters such as dielectric constant ( $\epsilon'$ ), dielectric loss ( $\epsilon''$ ), loss tangent ( $\tan\delta$ ), ac conductivity ( $\sigma_{ac}$ ) and complex electric modulus ( $M^*$ ) were obtained using admittance (capacitance and conductance) values measured in 10 kHz-5 MHz frequency range and 1 V-4 V positive voltage range. While the  $\epsilon'$  and  $\epsilon''$  value increase with decrease in frequency, the  $\sigma_{ac}$  value decreases. The values of real ( $M'$ ) and imaginary ( $M''$ ) part of complex modulus were obtained from the  $\epsilon'$  and  $\epsilon''$  values.  $M'$  value increases with increasing frequency and decrease with increasing voltage. The  $M''$  versus  $\log f$  plots indicate give a peak.

(Received March 30, 2019; accepted June 16, 2020)

**Keywords:** MPS structure, Complex dielectric and electric modulus, Electrical conductivity, Frequency effect

## 1. Introduction

In recent years, many scientists research electrical and dielectric properties of metal-polymer-semiconductor (MPS) structures with distinct polymer interlayers. They are believed that the polymer interlayer avoids inter-diffusion and reaction and leads these structures' performance in the respect of increase of dielectric constant and decrease of series resistance [1-10]. Particularly, the utilize of organic or polymer material at M/S interface become very appealing for the MPS structures because of their unique properties such as low cost, low weight, low conception energy and flexibility. Therefore, in recently, the MPS structures become more attractive in the application electronic and optoelectronic technology instead of MIS type structures.

Polymeric materials such as polypyrene (PPy), polyaniline (PANI) and especially polyvinyl alcohol (PVA) have been used as an organic interface layer. The PVA has an important place among organics/polymers which is a low cost and may be prepared by easy fabrication methods such as electro-spinning, electrostatic spraying, electrochemical deposition, sol-gel, dip coating, and spin coating [1-7]. In recent years, many of research about the modification of the metal-semiconductor (MS) structures with high-dielectric insulator, ferro-electric and metal-doped polymer materials are aiming to increase the specific capacitance under investigates [11-15] Also, the conductivity of polymers is weak, so pure PVA has a low dielectric constant. On the other hand, the interactions

between polymer chains can be developed the conductivity of polymer materials. Therefore, (Cu<sub>2</sub>O-CuO)-PVA composite materials are utilized as an essential material for electronic devices [6, 7].

The related relaxation mechanism and molecular orientation behaviour of the polymer and surface states are not fully understood yet, in spite of the dielectric characteristics of polymer has been researched. So, depending on frequency and biases, dielectric loss determination is a proper method for examining the polymer structure. In order to investigate the frequency-dependent dielectric properties, dielectric relaxation spectroscopy is used. Moreover, the analysis of the dielectric polarization and dielectric loss can be realized by utilizing this spectroscopy. The dielectric characteristics of materials depend on the frequency of the electrical field. All polarization mechanisms called as interfacial, dipolar, atomic and electronic polarization respond to an electrical field.

In present study, our aim is to investigate dielectric parameters ( $\epsilon'$ ,  $\epsilon''$  and  $\tan\delta$ ),  $\sigma_{ac}$ ,  $M'$  and  $M''$  of the MPS structure in the wide range of voltage and 10 kHz-5 MHz frequency interval. These properties of the structure were determined with using the admittance (capacitance-voltage and conductance-voltage) measurements.

## 2. Experimental details

The preparation of (Cu<sub>2</sub>O-CuO-PVA) composite material and the fabrication process of Au/(Cu<sub>2</sub>O-CuO-PVA)/n-Si (MPS) type SBDs were given in our previous study in detail [7]. The MPS type SBDs were fabricated on P-doped (n type Si) single crystalline Si wafer with (100) orientation, 0.2 Ω·cm resistivity and with approximately 300 μm thick. More information about these process and structure analysis X-ray diffraction (XRD) measurement and scanning electron microscopy (SEM) images) can be also seen in Ref. [7]. The capacitance and conductance measurements of this structure were carried out with utilizing a HP 4192A LF Impedance analyser at ordinary room temperature conditions. The calculations for ac conductivity and modulus and the dielectric characterization of the prepared MPS structure were made by utilizing these measurements.

## 3. Result and discussion

The ac conductivity, complex dielectric constant and complex electric modulus change with applied biases and frequency were calculated by using the capacitance-voltage-frequency (C-V-f) and conductance-voltage-frequency (G-V-f) measurements. These measurements were carried out in the frequency (10 kHz-5 MHz) and the applied biases (1-4 V) range. The C<sub>m</sub>-logf and G<sub>m</sub>-logf plots of the Au/(Cu<sub>2</sub>O-CuO-PVA)/n-Si (MPS) structure for distinct applied positive voltages were given in Fig. 1 and 2, respectively. As shown in these figures, both C<sub>m</sub> and G<sub>m</sub> values increase with the increasing applied positive voltage. However, the C<sub>m</sub> value decreases with increasing frequencies, while the G<sub>m</sub> value increases [16-18].

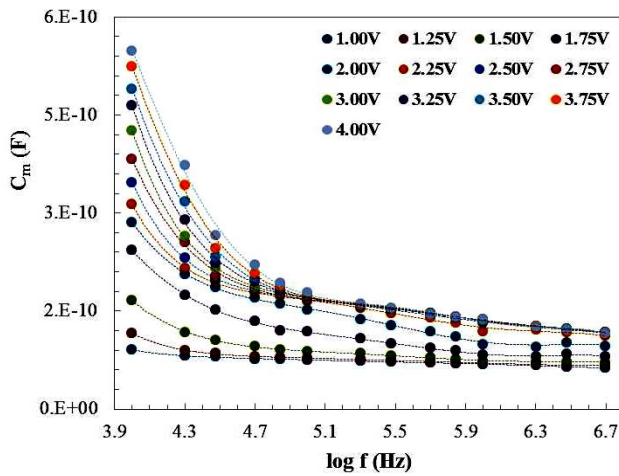


Fig. 1. The C<sub>m</sub>-logf plot of the MPS structure for distinct applied biases (color online)

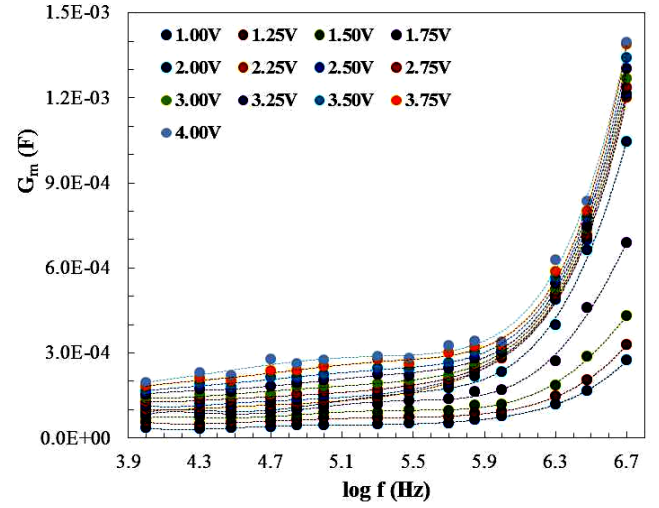


Fig. 2. The G<sub>m</sub>-logf plot of the MPS structure for distinct applied biases (color online)

The complex form of the complex permittivity ( $\epsilon^*$ ) was represented as below [19-23],

$$\epsilon^*(\omega) = \epsilon'(\omega) - i\epsilon''(\omega) \quad (1)$$

where  $\epsilon'$  is the real and  $\epsilon''$  is the imaginary part of the complex dielectric permittivity and as known the square root of -1 is denoted by  $i$ . The dipoles alignment strength in the dielectric is defined by  $\epsilon'$ , which is a dimension of the applied electric field's stored energy in the structure. Related with frictional dampening, the loss factor  $\epsilon''$  is known as the energy spent at dielectric that avoid bound charge displacements to be in phase with field alterations. The electrical and dielectric characteristics of structure can be certainly explained by complex permittivity and the  $\epsilon^*$  is given by,

$$\epsilon^* = \frac{Y^*}{i\omega C_0} = \frac{C}{C_0} - i \frac{G}{\omega C_0} \quad (2)$$

where  $Y^*$  is the admittance,  $G_m$  and  $C_m$  are the measured conductance and the capacitance values of dielectric materials at any bias voltage, respectively. The applied electric field's angular frequency is denoted by  $\omega$  and can be expressed as  $\omega=2\pi f$  [20]. Thus, the values  $\epsilon'$  and  $\epsilon''$  can be calculated from Eq. 2. as following:

$$\epsilon' = \frac{C}{C_0} \quad (3)$$

$$\epsilon'' = \frac{G}{\omega C_0} \quad (4)$$

where  $C_0$  is the empty capacitor's capacitance ( $C_0=\epsilon_0 A/d$ ),  $A$  is the rectifier contact's area ( $\text{cm}^2$ ),  $d$  is the thickness of

polymer layer and  $\epsilon_0$  is the free space charge's permittivity ( $8.85 \times 10^{-14}$  F.cm<sup>-1</sup>). The  $\tan \delta$  which is known as dissipation factor or loss tangent is the rate of is the rate of  $\epsilon'$  to the  $\epsilon''$  as follows.

$$\tan \delta = \frac{\epsilon''}{\epsilon'} \quad (5)$$

The ac electrical conductivity has been obtained from the  $\epsilon''$  values according to the equation [22-24],

$$\sigma^* = i\epsilon_0\omega\epsilon^* = i\epsilon_0\omega(\epsilon' - i\epsilon'') = \epsilon_0\omega\epsilon'' + i\epsilon_0\omega\epsilon' \quad (6)$$

So, the real part of  $\sigma^*$  is given by,

$$\sigma_{ac} = \omega\epsilon_0\epsilon'' \tan \delta = \epsilon_0\omega\epsilon'' \quad (7)$$

The  $\epsilon'$  and  $\epsilon''$  values were calculated from equation 3 and 4 by using the measured capacitance and conductance data. Then,  $\tan\delta$ , and  $\sigma_{ac}$  values were obtained from the calculated  $\epsilon'$  and  $\epsilon''$  data. The variations of dielectric parameters with frequency and biases in the depletion and accumulation regions were presented in Fig. 3 (a), (b) and (c). As shown in Fig. 3, the values of are  $\epsilon'$ ,  $\epsilon''$  and  $\tan \delta$  are extremely dependent on frequency and voltage.

$\epsilon'$ ,  $\epsilon''$  and  $\tan\delta$  parameters are generally increase with decreasing frequency and decreasing applied positive voltage. In addition, these alterations become considerably higher particularly at medium and lowest frequencies. Such behavior of them with frequency was attributed to less orientation times of the interface dipoles at alternating field direction and the surface states relaxation time. However, the dipoles which inside the dielectric polymer may ready for polarization under an electric field or applied biases that dislocates the charges from equilibrium position at low and medium frequencies. So, it can be say that, the consequence of the relaxation time is related with the dielectric parameters decrement by increasing frequencies [24-28].

The ac electrical conductivity ( $\sigma_{ac}$ ) alteration is illustrated in Fig. 4. As shown in the Fig. 4, the electrical conductivity ( $\sigma$ ) is almost independent of the frequency, but it increases exponentially with frequency for every bias that are corresponding to the ac and dc part of the  $\sigma$ . The space charge polarization is the reason of this increment and the charge accumulation formed at the polymer-semiconductor interface by decreasing frequencies. Therefore, at low frequencies the conductivity is low and almost independent of frequency [8, 26, 27].

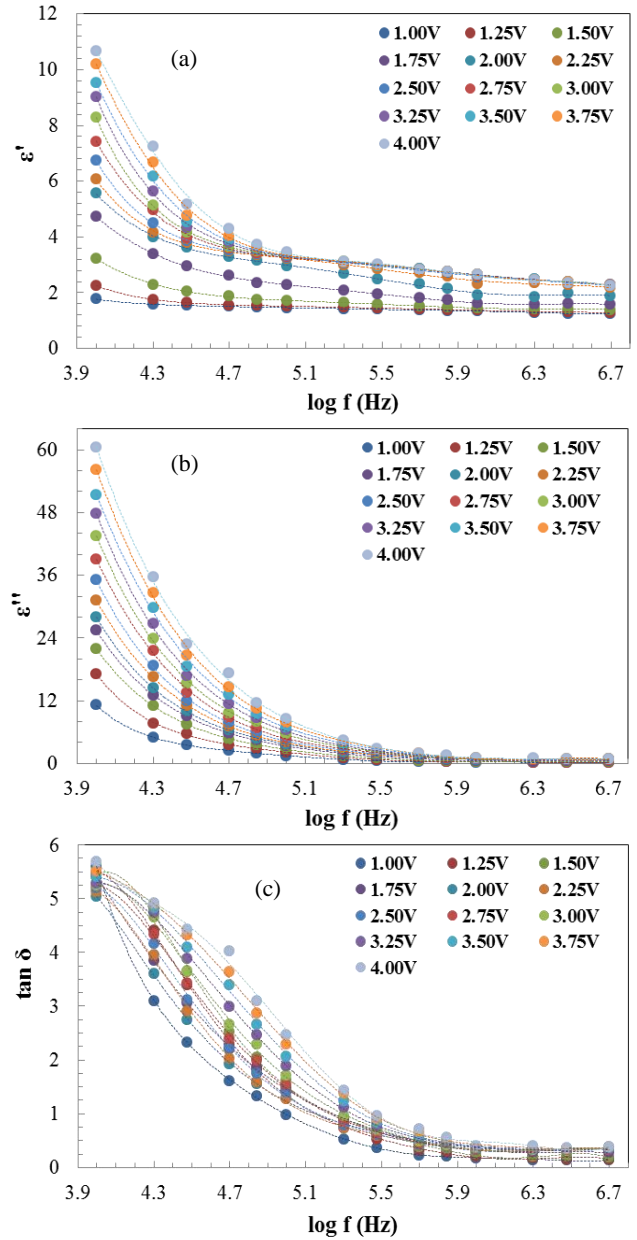


Fig. 3. The a)  $\epsilon'$ -logf, b)  $\epsilon''$ -logf and c)  $\tan\delta$ -logf plots of the MPS structure for various voltages (color online)

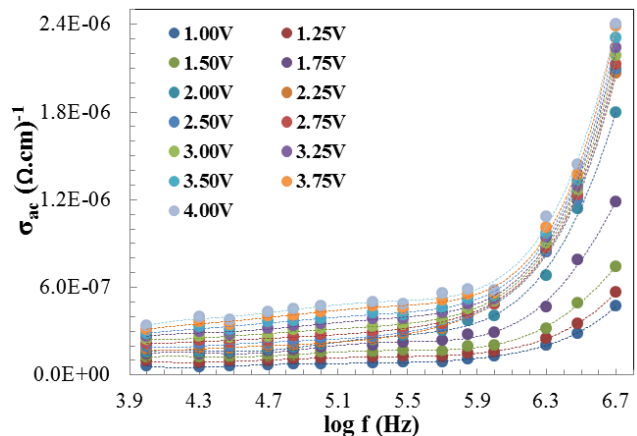


Fig. 4. The  $\sigma_{ac}$ -Inf plot of the MPS structure for various voltages (color online)

$$\sigma_{ac} = \omega C \tan \delta \left( \frac{d_i}{A} \right) = \varepsilon' 2\pi f \varepsilon_0 = B\omega^s \quad (0 < s < 1) \quad (8)$$

where, B and s are constants,  $\omega$  is angular frequency of the applied biases.

As seen in Eq.(8), dependent on frequency the increment in ac electrical conductivity is resulted from the carrier charges leaping from trap to other placed between polymer layer and Si in the semiconductor's forbidden band-gap. The double logarithmic  $\sigma_{ac}$ -f plots were drawn for various applied voltages for moderate and high frequencies which corresponds the ac electrical conductivity and illustrated in Fig. 5. This plot gives a linear behavior for each voltage. The measured slopes, which are s values, were calculated in the range of characterizing hopping conduction (0.11-0.24) [10, 28].

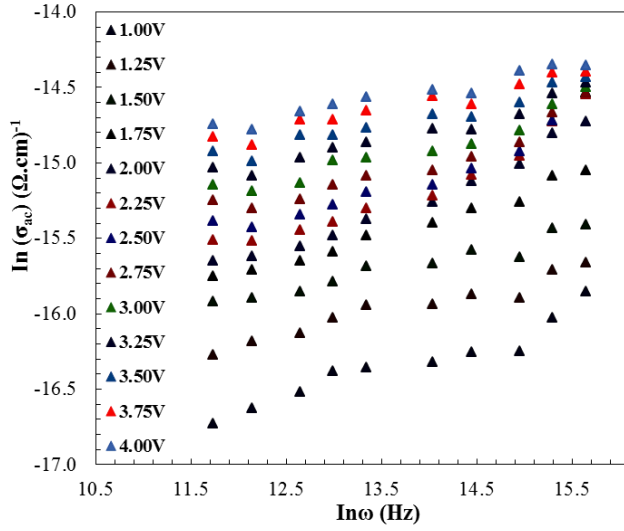


Fig. 5. The  $\ln\sigma_{ac}$ - $\ln\omega$  plots of the MPS structure for distinct applied biases (color online)

The examination of electrical response can be realized through complex electric modulus ( $M^*$ ) formalism. The below equation gives the complex electric modulus [21,22],

$$M^*(\omega) = \frac{1}{\varepsilon^*} = M'(\omega) + iM''(\omega) \quad (9)$$

In Eq. 9, complex electric modulus ( $M^*$ ) real and imaginary parts are denoted as  $M'$  and  $M''$ , respectively. The energy loss measurement of the material under electric field is denoted by  $M''$ .  $M'$  and  $M''$  can be derived by the following equations [21, 22]:

$$M'(\omega) = \frac{\varepsilon'(\omega)}{\varepsilon'(\omega)^2 + \varepsilon''(\omega)^2} \quad (10)$$

$$M''(\omega) = \frac{\varepsilon''(\omega)}{\varepsilon'(\omega)^2 + \varepsilon''(\omega)^2} \quad (11)$$

The  $M'$  and  $M''$  values were derived from Eq. 10 and 11 with using the obtained experimental values of  $\varepsilon'$ ,  $\varepsilon''$  and the variations of them were given in Fig. 6 and 7, respectively.

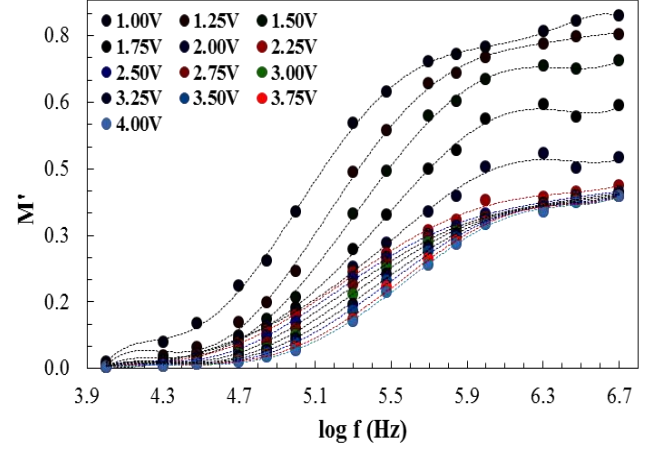


Fig. 6. The  $M'$ -logf plot of the MPS structure for various voltages (color online)

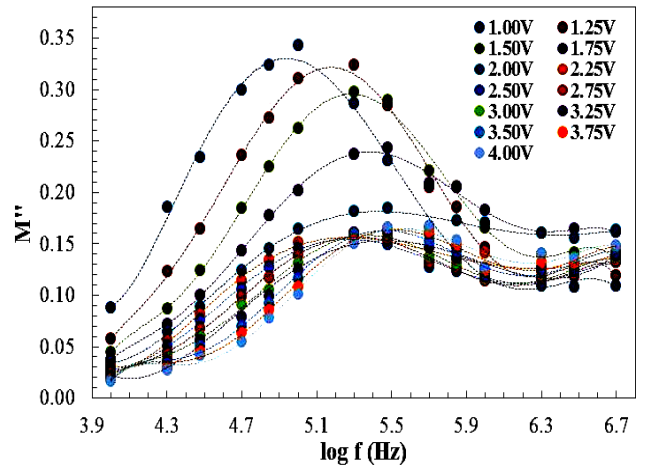


Fig. 7. The  $M''$ -logf plot of the MPS structure for distinct biases (color online)

It is obviously indicated in Fig. 6 and 7 that, both  $M'$  and  $M''$  values are strong function of voltage and frequency. The  $M'$  values increase with increasing frequency and decrease with increasing voltage. The  $M''$  values exhibit a peak and the magnitude of this peak increases with the decrement in voltage and its position shifts towards to low frequency. Such behaviours of these plots can be ascribed by the charges in traps and the relaxation polarization in doped polymers [17, 29-37].

#### 4. Conclusion

The impedance or admittance ( $Z=1/Y$ ) measurement depends on measuring the capacitance ( $C_m$ ) and conductance ( $G_m$ ) of a MPS structure as a function of applied biases and frequency is similar to the MIS type structure. Therefore, the dielectric characteristics of the fabricated Au/(Cu<sub>2</sub>O-CuO-PVA)/n-Si (MPS) structure have been studied by using the  $C_m$ -logf and  $G_m$ -logf characteristics. The  $\epsilon'$ ,  $\epsilon''$  and  $\tan \delta$  values decrease with frequency and decreasing applied positive voltage. The decrement of  $\epsilon'$  and  $\epsilon''$  with increase of frequency was based on the surface states and interfacial polarization. In other words, the increase in the values of  $\epsilon'$  and  $\epsilon''$  with respect to the charge storage in the traps can be explained by the increase of C and G with decreasing frequencies. Because, depending on the relaxation times, the charges or dipoles can be reconstituted and reordering under electric field. In addition, the polymer interlayer can handily polarize under an external electric field that dislocates the charges from equilibrium state. Moreover, in consequence of relaxation phenomenon which arises from the interfacial polarization and mobile charge carriers,  $\sigma_{ac}$  value increases with increased frequency. Finally, the M' and M'' values were obtained from the  $\epsilon'$ ,  $\epsilon''$  values. As results, the plots characteristics can be ascribed by the relaxation polarization in doped polymers and charges in traps. In conclusion, the obtained dielectric constant of (Cu<sub>2</sub>O-CuO-PVA) polymer layer is considerably higher from the conventional SiO<sub>2</sub> even at 10 kHz. In summary, these obtained results were shown that the capacitance high values can be provide with utilizing proper high-dielectric polymer between metal and semiconductor in place of traditional low-constant insulator interlayer such as SnO<sub>2</sub> and SiO<sub>2</sub>. It may be utilized in a large variety of applications on charges/energy capture and storage.

#### Acknowledgements

This study was supported by Gazi University Scientific Research Project. (Project Number: GU-BAP.05/2019-26).

#### References

- [1] L. W. Lim, F. Aziz, F. F. Muhammad, A. Supangat, K. Sulaiman, *Synthetic Metals* **221**, 169 (2016).
- [2] A. Srinivasan, S. Bandyopadhyay, *Advances in Polymer Materials and Technology*, CRC, Boca Raton, 2017.
- [3] J. Kwon, *J. Polym. Sci. A Polym. Chem.* **49**, 1119 (2011).
- [4] V. Tamilavan, P. Sakthivel, Y. Li, M. Song, C. H. Kim, S. H. Jin, M. H. Hyun, *J. Polym. Sci. A Polym. Chem.* **48**, 3169 (2010).
- [5] G. Ersöz, İ. Yücedağ, Y. Azizian-Kalandaragh, İ. Orak, Ş. Altındal, *IEEE Trans. Electron Dev.* **63**, 2948 (2016).
- [6] M. Sharma, S. K. Tripathi, *Mater. Sci. Semi. Process* **41**, 155 (2016).
- [7] A. Büyükbaş-Uluşan, A. Tataroğlu, Y. Azizian-Kalandaragh, Ş. Altındal, *J. Mater. Sci.: Mater. Electron.* **29**, 159 (2018).
- [8] İ. Taşcıoğlu, Ö. Tüzün Özmen, H. M. Şağban, E. Yağlıoğlu, Ş. Altındal, *J. Electron. Mater.* **46**, 2379 (2017).
- [9] S. Demirezen, A. Kaya, S. A. Yerişkin, M. Balbaşı, İ. Uslu, *Results Phys.* **6**, 180 (2016).
- [10] Ç. Bilkan, Y. Azizian-Kalandaragh, Ş. Altındal, R. Shokrani-Havigh, *Physica B* **500**, 154 (2016).
- [11] R. Padma, B. P. Lakshmi, V. R. Reddy, *Superlattices Microstruct.* **60**, 358 (2013).
- [12] Y. Ş. Asar, T. Asar, Ş. Altındal, *J. Alloy. Comp.* **628**, 442 (2015).
- [13] A. Kaya, S. Alialy, S. Demirezen, M. Balbaşı, S. A. Yerişkin, A. Aytimur, *Ceram. Inter.* **42**, 3322 (2016).
- [14] M. Mümtaz, N. A. Khan, *Physica C* **469**, 728 (2009).
- [15] Asma M. Alturki, *J. Nanostructure Chem.* **8**, 153 (2018).
- [16] I. M. Afandiyeva, M. M. Bulbul, Ş. Altındal, S. Bengi, *Microelectron. Eng.* **93**, 50 (2012).
- [17] İ. Yücedağ, A. Kaya, Ş. Altındal, İ. Uslu, *Chin. Phys. B* **23**, 047304 (2014).
- [18] A. Tataroğlu, Ş. Altındal, *Microelectron. Eng.* **83**, 582 (2006).
- [19] D. Cheng, *Field and Wave Electromagnetics*, 2nd Ed., Addison-Wesley, New York, 1989.
- [20] M. Popescu, I. Bunget, *Physics of Solid Dielectrics*, Elsevier, Amsterdam, 1984.
- [21] A. Chelkowski, *Dielectric Physics*, Elsevier, Amsterdam, 1980.
- [22] C. P. Symth, *Dielectric Behaviour and Structure*, McGraw-Hill, New York, 1955.
- [23] Vera V. Daniel, *Dielectric Relaxation*, Academic Press, London, 1967.
- [24] T. Ataseven, A. Tataroğlu, T. Memmedli, S. Özçelik, *J. Optoelectron. Adv. M.* **14**, 640 (2012).
- [25] A. Buyukbas, A. Tataroğlu, *J. Nanoelectron. Optoelectron.* **10**, 675 (2015).
- [26] S. A. Yerişkin, M. Balbaşı, A. Tataroğlu, *J. App. Polymer Sci.* **133**, 43827 (2016).
- [27] A. Tataroğlu, *J. Optoelectronic. Adv. M.* **13**, 940 (2011).
- [28] B. Coşkun, *J. Mater. Electron. Dev.* **1**, 65 (2019).
- [29] S. Altındal Yerişkin, G. Ersöz, İ. Yücedağ, *J. Nanoelectron. Optoelectron.* **14**, 1126 (2019).
- [30] A. Tataroğlu, Ş. Altındal, *Microelectron. Eng.* **85**, 1866 (2008).
- [31] İ. Yücedağ, G. Ersöz, A. Gümüş, Ş. Altındal, *Inter. J. Modern Phys. B* **29**, 1550075 (2015).
- [32] A. Karabulut, A. Türüt, Ş. Karataş, *J. Molecular Structure* **1157**, 513 (2018).
- [33] S. Demirezen, *Appl. Phys. A* **112**, 827 (2013).
- [34] E. Efil, N. Kaymak, E. Seven, A. Tataroğlu, S. Bilge Ocak, E. Orhan, *Physica B* **568**, 31 (2019).
- [35] H. Tecimer, S. O. Tan, Ş. Altındal, *IEEE Trans. Electron. Dev.* **65**, 231 (2017).
- [36] S. O. Tan, H. Tecimer, O. Çiçek, *IEEE Trans. Electron. Dev.* **64**, 984 (2017).
- [37] A. Büyükbaş Uluşan, A. Tataroğlu, *Silicon* **10**, 2071 (2018).

\*Corresponding author: aysel.buyukbas@gmail.com